Online-Journals.org

iJOE International Journal of Online and Biomedical Engineering

iJOE | eISSN: 2626-8493 | Vol. 20 No. 5 (2024) | OPEN ACCESS

https://doi.org/10.3991/ijoe.v20i05.45609

PAPER

Post-Operative Brain MRI Resection Cavity Segmentation Model and Follow-Up Treatment Assistance

Sobha Xavier P(✉), Sathish P K, Raju G

Department of Computer Science, Christ (Deemed to be University), Bengaluru, Karnataka, India

sobha.xavier@res.christuniversity.in

ABSTRACT

Post-operative brain magnetic resonance imaging (MRI) segmentation is inherently challenging due to the diverse patterns in brain tissue, which makes it difficult to accurately identify resected areas. Therefore, there is a crucial need for a precise segmentation model. Due to the scarcity of post-operative brain MRI scans, it is not feasible to use complex models that require a large amount of training data. This paper introduces an innovative approach for accurately segmenting and quantifying post-operative brain resection cavities in MRI scans. The proposed model, named Attention-Enhanced VGG-U-Net, integrates VGG16 initial weights in the encoder section and incorporates a self-attention module in the decoder, offering improved accuracy for postoperative brain MRI segmentation. The attention mechanism enhances its accuracy by concentrating on a specific area of interest. The VGG16 model is comparatively lightweight, has pre-trained weights, and allows the model to extract incredibly detailed information from the input. The model is trained on publicly available post-operative brain MRI data and achieved a Dice coefficient value of 0.893. The model is then assessed using a clinical dataset of postoperative brain MRIs. The model facilitates the quantification of the resected regions and enables comparisons with each brain region based on pre-operative images. The capabilities of the model assist radiologists in evaluating surgical success and directing follow-up procedures.

KEYWORDS

Attention-Enabled U-Net, post-operative magnetic resonance imaging (MRI), resection cavities, segmentation, VGG16 encoder

1 INTRODUCTION

Surgical interventions on the brain often involve the resection of abnormal tissue, leading to the formation of cavities [1]. The precise segmentation of resection cavities in post-operative brain magnetic resonance imaging (MRI) is essential for assessing surgical efficacy, predicting patient outcomes, and comprehending the

Xavier, P.S., Sathish, P.K., Raju, G. (2024). Post-Operative Brain MRI Resection Cavity Segmentation Model and Follow-Up Treatment Assistance. *International Journal of Online and Biomedical Engineering (iJOE)*, 20(5), pp. 133–149. https://doi.org/10.3991/ijoe.v20i05.45609

Article submitted 2023-10-06. Revision uploaded 2023-12-20. Final acceptance 2023-12-20.

anatomical changes resulting from the procedure [2]. The major challenge in the context of post-operative brain MRI is obtaining annotated data, which is often limited due to ethical and practical considerations. So, there is a need to develop a model that can perform well even with a limited amount of data. The model should be able to capture small details from the available dataset. At the same time, the model should be kept simple to prevent overfitting when dealing with a small dataset. Manual segmentation by an expert is time-consuming and may be prone to errors. Traditional image processing methods for MRI segmentation often struggle to achieve high precision due to the complex and variable nature of brain tissue [3].

In recent years, deep learning techniques have shown remarkable promise in medical image segmentation tasks. Recent research on deep learning models for medical image segmentation includes efficient models such as the Residual Full Convolutional Network (ResFCNET) [4]. It is a skin lesion recognition model that combines residual learning and a full convolutional network to perform semantic segmentation of skin lesions. Additionally, pre-trained models such as VGG-16, ResNet-50, and AlexNet [5] are utilized to enhance performance, along with modified U-Net architectures [6]. Among these, the U-Net architecture has gained prominence for its ability to effectively capture spatial information [7, 8]. However, the success of deep learning models, such as U-Net, depends on the availability of large labelled datasets [9]. In the context of postoperative brain MRI segmentation, only a limited number of standard datasets are available. To address this limitation, incorporating the pre-trained weights of the VGG16 model as the encoder part and utilizing an attention mechanism [10, 11] to capture fine details from the dataset is a better choice. The study begins with an exploration of existing post-operative brain MRI segmentation models. Then, a publicly available dataset is acquired. From the study on existing models, the U-Net model performed the best. This highlights the importance of choosing the appropriate deep learning architecture when working with limited datasets. Next, we explored various pre-trained backbones for the U-Net model, such as ResNet, DenseNet, MobileNet, EfficientNet, and VGG16 [12, 13, 14], which are effective choices for medical image segmentation tasks. Studies show that VGG16 and MobileNet are often considered more suitable for U-Net when dealing with limited datasets [9, 15]. The simplicity of VGG16's architecture and the efficiency of MobileNet's design make them well-suited for effectively handling small datasets in medical image segmentation tasks.

In this study, several existing image segmentation models were experimented with, including the U-Net model, Attention U-Net model, U-Net with a VGG16 backbone, and U-Net with a ResNet backbone. Upon comparing the results of these models, it was found that the attention mechanism significantly improved the model's accuracy. VGG16 offers a simpler architecture compared to ResNet50. Given the small dataset size, it is observed that U-Net with a VGG16 backbone outperforms U-Net with a ResNet50 model. In their study, Gharaibeh et al. [16] efficiently extracted brain features using a Multi-Scale Feature Pyramid Fusion Module with VGG16 (MSFP-VGG16). This approach enhances both detection and classification accuracy. This insight leads to the proposal of a novel model that combines the features of U-Net, an attention mechanism, and a trained VGG16 model.

The primary objective of this research is to provide valuable support for the post-treatment monitoring of brain tumor patients. It is important to accurately segment the resection cavity after surgery and quantify postoperative brain resection

cavities in MRI scans. Additionally, a critical aspect is to compare pre- and postoperative MRI images to determine whether the tumor has been completely removed. This comparison is a crucial step in assessing surgical outcomes and planning follow-up treatments. In this paper, we present a comprehensive analysis of pre- and post-operative brain MRI in two parts. The first part introduces an automated brain resection cavity segmentation model designed to accurately segment the cavity. The proposed model utilizes an attention-enhanced U-Net with a VGG16 encoder to improve the accuracy of cavity segmentation. The proposed model demonstrates superior accuracy with an IoU of 0.890 and a Dice coefficient of 0.893 compared to other U-Net variations. The second part involves a volumetric analysis of pre- and post-operative brain MRI scans, providing insights into surgical effects and follow-up treatments.

2 RELATED WORK

Postoperative cavity segmentation in brain MRI is a crucial task in the field of medical image analysis, assisting clinicians in accurately identifying and assessing surgical sites. Notable contributions have been made to this area over the years, with each offering innovative methods to improve the accuracy and efficiency of postoperative cavity segmentation. Significant contributions have emerged in the field of postoperative brain MRI segmentation between 2016 and 2022. Innovations include Ke Zeng et al.'s "GLISTRboost" [17] (2016), Alain Jungo's "Fully convolutional DenseNet" [18] (2018), Ken Chang's "3D U-Net" [19] (2019), Pérez-García et al.'s "Self-supervised 3D CNN" [20] (2021), Lotan et al.'s "Autoencoder regularization-cascaded anisotropic CNN model" [21] (2022), Holtzman et al.'s "Neural Network U-Net (NNU-Net)" [22] (2022), Ramesh et al.'s "Post-Surgical Brain Tumor Segmentation Model" [23] (2023), Campbell Arnold et al.'s "Modified U-Net model" [2] (2022), and Mina Ghaffari et al.'s "Transfer learning method" [24] (2022). These contributions showcase the evolution of techniques and models, enhancing the accuracy of postoperative brain MRI segmentation.

In their study, Pérez-García et al. [20] introduce a novel method for accurately segmenting brain resection cavities using CNNs and self-supervised learning. This approach achieves high DSC values for real resections on postoperative MRI scans. Trained initially with simulated resections, the model achieves Dice Similarity Coefficient (DSC) values between 74.9 and 82.4 across datasets. After fine-tuning, the DSC values improved to 80.2–89.2. Human annotators' inter-rater agreement stands at 84.0, serving as a benchmark. EPISURG, a self-supervised resection segmentation classifier exclusively trained on simulated data, demonstrates substantial improvement. Achieving a median DSC of 0.805 using simulated resections, it outperforms a classifier trained with manual labels (median DSC of 0.653). Despite advancements, false negatives persist, attributed to missing features in simulated data. Further refinement is highlighted to enhance accuracy. The study highlights the effectiveness of self-supervised learning and simulated data in improving resection cavity segmentation accuracy [20].

Campbell Arnold et al. [2] present an innovative approach to segmenting brain resection cavities in postoperative MRI scans of epilepsy patients. The method employs an automated segmentation algorithm integrated into a user-friendly graphical user interface (GUI), estimating brain volumes and assisting in clinical assessments. The algorithm utilizes an ensemble of U-Net networks trained on

various slices, yielding promising results. The median DSC values are 0.84 and 0.74 for cross-validation and held-out test sets, respectively, indicating good inter-rater reliability among radiologists. However, the study acknowledges limitations such as strict inclusion criteria, limited representation of the surgical approach, and reliance on a single rater. The study highlights the potential while emphasizing the need to address limitations for improved postoperative brain volume quantification.

Billardello et al. [25] focus on accurately delineating resected brain cavities in MRI scans of patients undergoing epilepsy surgery. They propose a semi-automated segmentation pipeline using postoperative MRIs from 35 patients. The developed region-growing algorithm achieves a DSC of 0.83 for segmentation accuracy. Limitations include incompatibility with laser ablation cases and the need for further development. Despite these limitations, their approach shows promise for identifying biomarkers of the epileptogenic zone, which can benefit both research and clinical applications. The text highlights the limitations of manual tracing and region-growing algorithms for delineating brain cavities in MRI scans for epilepsy surgery, addressing issues related to subjectivity and sensitivity.

In the work of Ghaffari et al. [24], the challenge of automated brain tumour segmentation from post-operative images is addressed. The study introduces an automated method for segmenting brain tumours into sub regions using a 3D densely connected U-net model. The dataset comprises multimodal post-operative brain scans of 15 patients who underwent radiation therapy, along with manual annotations. The model demonstrates dice scores of 0.90, 0.83, and 0.78 for predicting the whole tumour, tumour core, and enhancing tumour sub regions on the BraTS20 blind validation dataset. Despite the small dataset size, the model achieves dice scores of 0.83, 0.77, and 0.60 for the corresponding subregions. Limitations include performance discrepancies between local and BraTS datasets, especially in the enhancing core subregion, attributed to dataset characteristics and class imbalance. The study also acknowledges the influence of expert raters on annotations and proposes potential areas for future enhancements.

Casseb et al. introduced ResectVol [26], a tool for segmenting surgical cavities in postoperative MRI images of epilepsy patients. Using a MATLAB-based pipeline, it generates 3D masks and estimates lacuna volume. Validation involved comparing manual and automated segmentations from 51 MRI scans, resulting in the ResectVol tool with a median dice similarity coefficient of 0.77. ResectVol is significant in epilepsy surgery, offering automated segmentation to mitigate bias and align resected regions with preoperative findings. However, patients who underwent postoperative MRI within five months were excluded due to segmentation challenges near blood, gliosis, and edema. The algorithm intentionally overestimates slightly for comprehensive detection. ResectVol's performance relies on tissue contrast, favouring higher-contrast images.

In essence, the scarcity of postoperative MRI datasets for segmenting brain resection cavities poses a significant challenge. Current research in this field is limited, and some studies utilize self-supervised or transfer learning methods within the U-Net model to address this issue, achieving a maximum reported dice score of 0.84. In response to this, our work aims to enhance the segmentation capabilities of the U-net model by integrating the initial weights of VGG16 in the encoder section and a self-attention module in the decoder section. This module recalibrates feature maps

by assigning varying levels of attention to different spatial regions. Consequently, the model refines its predictions during the up-sampling process, prioritizing specific features learned in the encoding phase. This focused attention in the decoder enhances the model's ability to capture intricate details, which are essential for accurate segmentation.

3 MATERIALS AND METHODS

3.1 Dataset

EPISURG dataset. In their study, Pérez-García et al. [20] introduced the EPISURG dataset, which is a collection of T1-weighted MRI scans from 430 patients who underwent respective brain surgery for epilepsy at the National Hospital of Neurology and Neurosurgery (Queen Square, London, United Kingdom) between 1990 and 2018. The dataset was segmented by three human raters, each working on partially overlapping subsets of EPISURG. However, the dataset has certain limitations. While there are 430 postoperative MRI scans available, corresponding preoperative MRI scans are only available for 268 subjects. Only a limited number of ground-truth images for the resection cavities are available. As a result, a subset of 37 subjects with complete and accurate data was selected and prepared for further analysis. This subset contains both pre-operative and post-operative data, including information about hemispheres, types of surgery, planned surgeries, emergency surgeries, and agreement among raters. This subset of the EPISURG dataset holds particular significance for understanding the impacts of brain surgeries through pre-operative and post-operative information.

Clinical dataset. Ten patients' worth of data were gathered for the clinical dataset in January 2023 from the MRI Diagnostic Centre in Kerala. Post-operative brain MRI scans using T1 and T2 imaging modalities are included in this dataset. The data was converted from the DICOM format to the NIfTI format. Selected DICOM-formatted slices from the clinical dataset are shown in Figure 1.

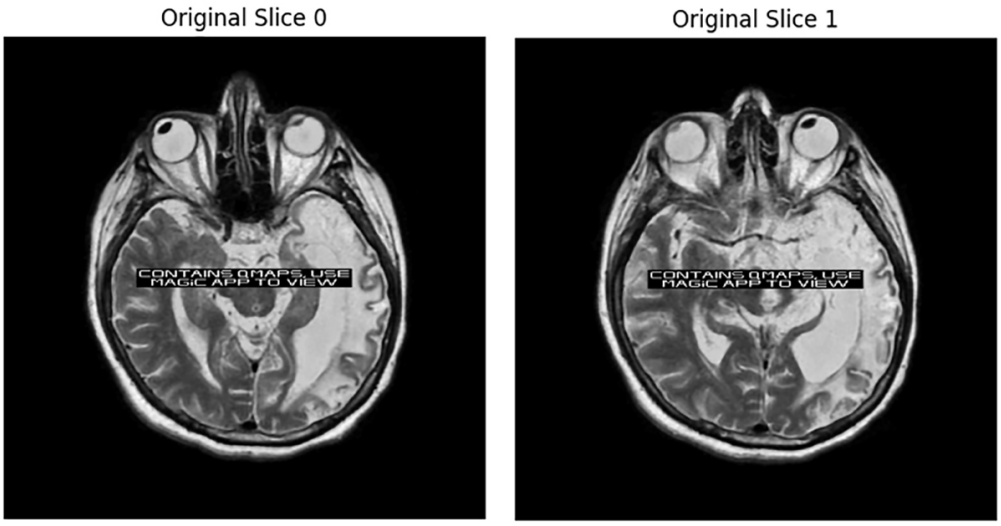

Fig. 1. *(Continued)*

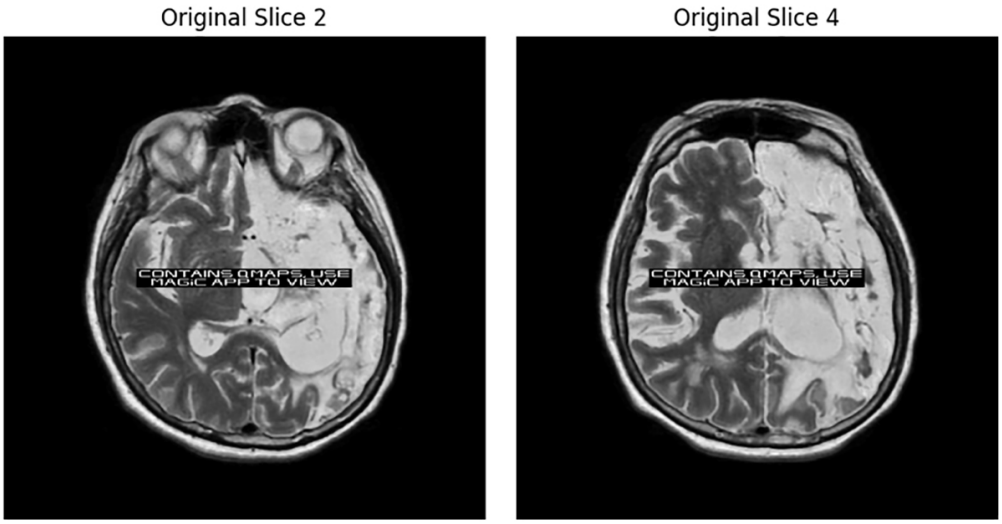

Fig. 1. Chosen slices from the clinical dataset

3.2 Data preprocessing

This section provides an overview of the customized preprocessing steps and data augmentation techniques used in this study. Two different post-operative brain MRI datasets were used in the study: the EPISURG dataset for cavity segmentation training [20], as well as a limited collection of clinical datasets to evaluate the performance of the model. The clinical dataset was provided in DICOM format and included complete skull information.

The initial preprocessing involved combining various time slices from the DICOM files into a consolidated .nii.gz (NIfTI) format. To facilitate this transformation, the SimpleITK package is utilized [27]. Subsequently, the region of interest is extracted by cropping out specific areas from the complete skull. To provide a comprehensive visual representation, the results of each enhancement method are depicted in Figures 2a and b. Figure 2a illustrates the consolidated NIfTI (Neuroimaging Informatics Technology Initiative) image, and Figure 2b. This image showcases a cropped region of interest (ROI) within the brain anatomy. This selected area of focus is essential for targeted analysis and segmentation processes, enabling precise examination of specific anatomical features or pathological regions.

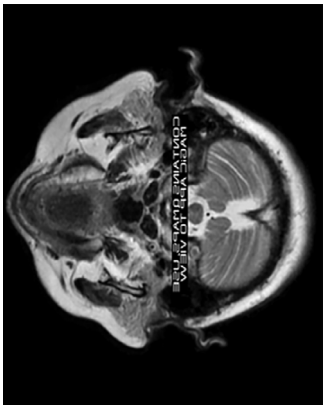

Fig. 2a. Consolidated NIfTI image

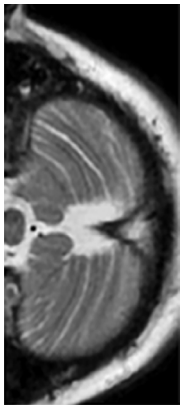

Fig. 2b. Cropped region of interest

3.3 End-to-end model flow

In this paper, we introduce an end-to-end model flow designed to accurately segment resection cavities and compare pre- and post-operative MRI images. This comprehensive analysis involves two parts: the first part automates the segmentation of resected areas in postoperative brain MRIs, and the second part enables the comparison of preoperative and postoperative brain MRIs. These functionalities provide a comprehensive reference for radiologists to evaluate surgical outcomes and inform subsequent treatments. Figure 3 depicts the entire workflow of the proposed model.

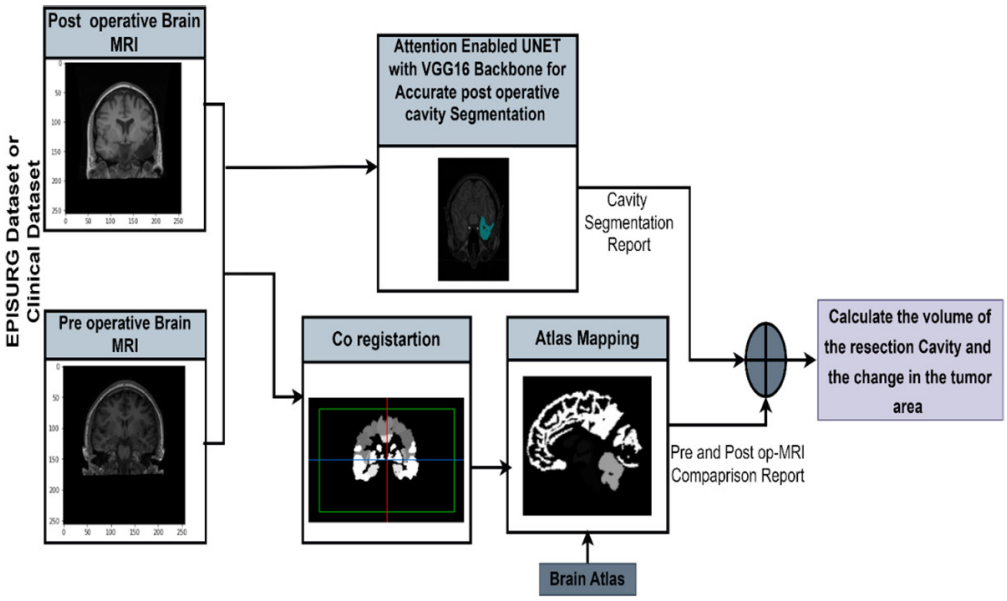

Fig. 3. End-to-end model flow: resection cavity segmentation and comparative analysis of pre- and post-operative MRI

3.4 Comparative benchmark models and proposed framework

This study tested several existing image segmentation models, including the U-Net model, the Attention U-Net model, the VGG16 backbone U-Net, and the ResNet backbone U-Net. These applications illuminate our findings, highlighting the significant improvement in model accuracy due to the attention mechanism. It was also observed that, considering the small size of the dataset, VGG16 offers a simpler architecture than ResNet50. Additionally, U-Net using a VGG16 backbone outperformed U-Net utilizing a ResNet50 model. As a result of this observation, a unique model was proposed. The model combines a trained VGG16 model, an attention mechanism, and U-Net features. An outline of the research architecture and specifics regarding the suggested model are provided in the following sections.

Attention-based U-Net. Gitonga [28] proposed a 3D attention-based U-Net architecture for accurate brain tumor segmentation by combining multi-modal MRI volumes. The incorporation of an attention mechanism in the decoder of U-Net

enhances segmentation accuracy by highlighting malignant tissues and downplaying healthy ones. The model implementation takes an input volume of 224 × 224 × 54 and produces an output volume of 64 × 32 × 32. It includes an encoder that uses 3D convolutional layers to extract hierarchical features from the input data. The decoder, consisting of extra convolutional layers, upscales the encoded features to produce the final segmentation mask. Additionally, the model integrates an attention mechanism, enhancing its capacity to focus on relevant spatial regions for improved segmentation precision.

U-Net with VGG16 backbone. Pravitasari et al. [29] introduced U-Net-VGG16, a modified architecture for MRI-based brain tumor segmentation. They achieved this by converting VGG16 into a U-Net architecture through the addition of an expansive layer, creating a symmetrical "U" shape. The U-Net-VGG16 model combines the U-Net and VGG16 architectures for image segmentation. It employs an encoder based on VGG16 to capture hierarchical features by progressively reducing spatial dimensions. The decoder, following the U-Net pattern, then upscales these features to generate the segmentation mask.

U-Net with ResNet50 backbone. In their paper, Asiri et al. [30] present a CNN model that combines fine-tuned ResNet50 and U-net architectures for accurate brain tumor classification and detection in MRI images. The fine-tuned ResNet50 excels in tumor detection, while U-net precisely segments tumors. The U-Net-ResNet50 model combines the U-Net architecture with the ResNet50 convolutional neural network as its backbone for image segmentation tasks. It takes an input image and utilizes ResNet50's deep residual layers in the encoder to efficiently capture multi-scale features. In the decoder, following the U-Net structure, it upscales and combines these features to generate the segmentation mask.

The architecture of proposed segmentation model. To develop an efficient model for the automatic segmentation of resected regions in postoperative brain MRI, a model named the Attention-Enhanced VGG-U-Net is proposed. This model integrates a self-attention module into the U-Net decoder, enhancing feature maps by assigning varying levels of attention to specific spatial regions. In contrast to applying attention mechanisms across both the encoding and decoding phases, the focus is exclusively on the decoder. The pre-trained knowledge from VGG16 on a larger dataset adapts well, enhancing the encoder and overall model adaptation. Figure 4 showcases the detailed architecture of the proposed model for automatic postoperative resection cavity segmentation. The diagram illustrates the arrangement of convolutional layers, skip connections, and attention modules within the U-Net framework, enhanced by the integration of the VGG16 backbone. The architecture begins with an input size of 224 × 224 × 54, representing the initial image with 54 feature channels. Through successive convolutional layers and max-pooling operations, the dimensions reduce to 112 × 112 × 128 and subsequently to 28 × 28 × 512 in the encoder. The dense block is used for feature extraction and representation. This architecture is designed for robust feature extraction, attention-guided decoding, and precise segmentation tasks. Figure 4b provides a detailed illustration of the Attention Module utilized in the Attention-Enabled U-Net architecture. This module is responsible for recalibrating feature maps by assigning varying levels of attention to different spatial regions, ensuring that the network focuses on critical details during the segmentation process. Figure 4c visually represents the internal workings and flow of information within the attention module.

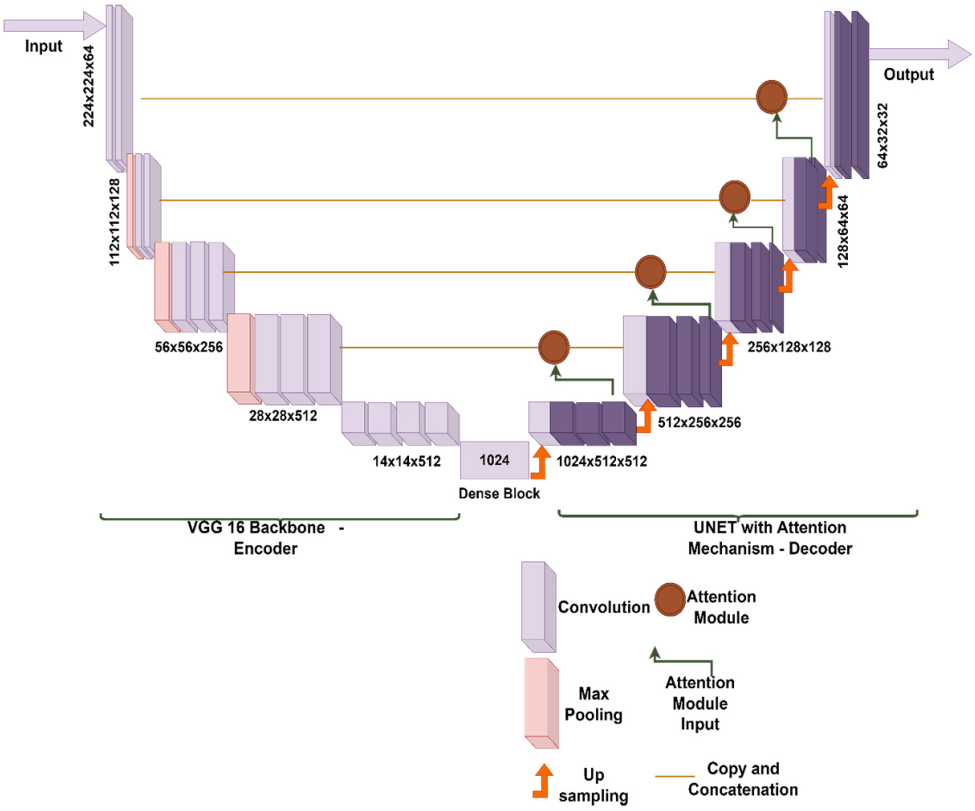

Fig. 4a. The architecture of attention-enabled U-Net with VGG16 backbone

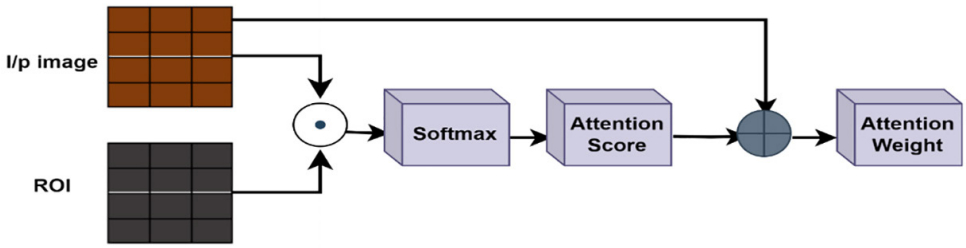

Fig. 4b. Attention module

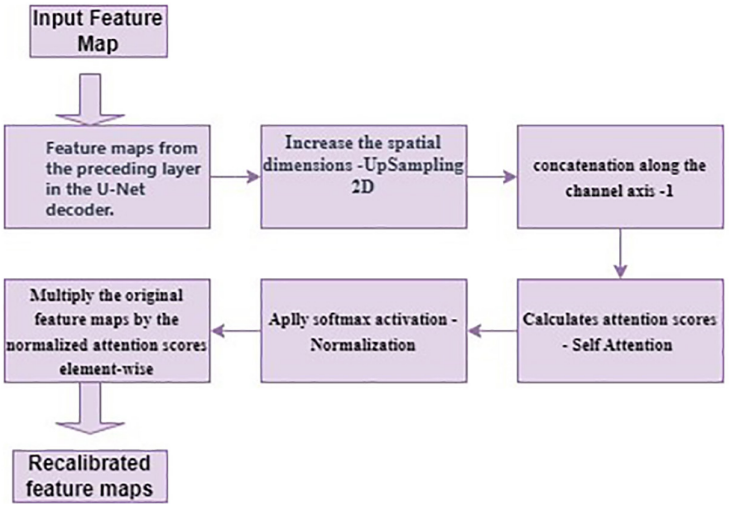

Fig. 4c. The internal workings and flow of information within the self-attention module

4 EXPERIMENTAL SETUP

4.1 Experimental setup of segmentation model

The primary goal of this research is to propose a model for accurately segmenting the resection cavity in postoperative brain MRI. As part of our experiments, we assessed the performance of various segmentation models for medical imaging. The conventional U-Net model exhibited an IOU of 0.67 and a dice coefficient of 0.72. In contrast, the U-Net model attracted significantly improved performance, achieving an IOU of 0.8373 and a Dice coefficient of 0.8255. This underscores the enhanced efficiency provided by the attention mechanism. Prior studies suggest that incorporating a pre-trained backbone into the U-Net model can enhance efficiency. In pursuit of this goal, we chose to use the U-Net with ResNet50. Unfortunately, this model experienced overfitting issues due to the limited dataset and its deep architecture, with accuracy plateauing at 0.1 after the 5th epoch. Subsequently, we experimented with the U-Net model using the VGG16 backbone, which resulted in an IOU of 0.7934 and a Dice coefficient of 0.7752. While this model outperformed the conventional U-Net model, it still fell short of the performance achieved by the attention U-Net model.

Finally, the proposed model that was tested is an attention-enhanced U-Net with a VGG16 backbone. It outperformed all other implemented models with an IOU of 0.8901 and a Dice coefficient of 0.8933. VGG16 is simple and has fewer parameters, making it suitable for better stability with small datasets. The integration of attention mechanisms in alignment with VGG16 improved the effectiveness of the segmentation process. For training, a configuration of 30 epochs was employed, utilizing the Adam optimizer with a reduced batch size of four and incorporating layer normalization instead of batch normalization. This approach better addresses overfitting concerns, yielding a dice coefficient of 0.8522 with the small dataset. The experiment involved processing 3D input MRI slices using the loaded model. To enhance model adaptability, data augmentation techniques were incorporated during training, following the approach proposed by Campbell Arnold et al. [2], Perez-García et al. [20]. These techniques included random flips and rotations of up to 10 degrees, enhancing the dice coefficient, which increased to 0.8933. Simultaneously, the loss function steadily decreased from 0.831 to 0.037 during training. Figure 5 provides a comprehensive summary of the training results for the proposed model.

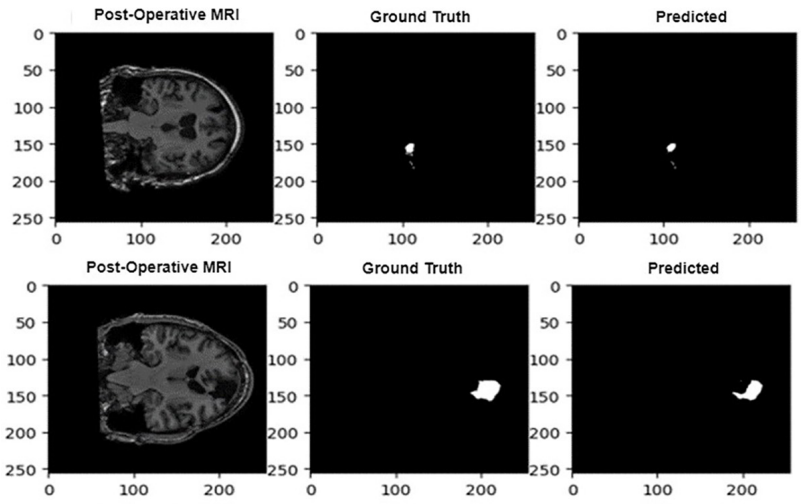

Fig. 5. *(Continued)*

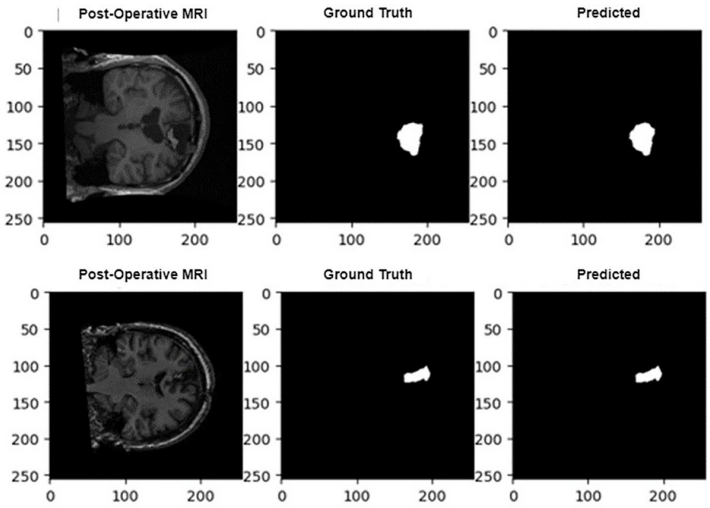

Fig. 5. Training results of the proposed model on EPISURG dataset

4.2 Experimental setup of pre and post operative brain MRI comparison

To compare preoperative and postoperative brain MRIs, a non-diffeomorphic registration [31] of preoperative and postoperative images is performed. The approach specified in Campbell Arnold et al.'s [2] study using the Ants library was followed for this research. The image registration process involves aligning the pre-operative image with the post-operative image by applying an affine transformation. This registration utilizes the SyN transformation to align preoperative images with the postoperative space. Subsequently, an Atlas segmentation is generated from the pre-operative image using the Antspynet library and applying the Desikan-Killiany-Tourville (DKT) [32] labelling scheme. Afterward, the postoperative MRI images were processed, with masks outlining resected regions and an atlas defining brain areas. By combining the mask and atlas, the regions affected by surgery are isolated. The computed volume of resected tissue quantifies the surgical impact. To calculate the percentage of volume resected for each ROI, a simple image processing technique called element-wise multiplication (or pixel-wise multiplication) is used. This technique involves multiplying the corresponding pixel or voxel values of the mask (representing the resected region) and the atlas data. This element-wise multiplication effectively isolates the regions contained within the resection zone, highlighting the areas of interest in the combined image. Atlas mappings linked pixel values to ROI names. For each ROI, the calculated percentage of remaining tissue summarizes surgical outcomes. These steps allowed us to assess resected tissue volumes across distinct brain regions and visualize the resected areas. The results of the comparison between preoperative and postoperative brain MRI images are depicted in Figure 6.

```
Pre- and Post-operative MRI comparison and Volumetric report!!!!

Resection results, by region:
Total resection volume (cubic cm): 9.783331157430414

right entorhinal        : 95.824% remaining
right fusiform          : 96.213% remaining
right inferior temporal : 76.04599999999999% remaining
right middle temporal   : 80.057% remaining
right Para hippocampal  : 98.565% remaining
right superior temporal : 90.679% remaining
```

Fig. 6. Brain MRI comparison between pre- and post-operative states with report on volumetric difference calculation

5 RESULTS AND DISCUSSIONS

5.1 Performance measure

Performance is evaluated on the test dataset (EPISURG) using two widely utilized metrics: IoU and the dice coefficient [31]. The IoU measures the overlap between the predicted segmentation and the ground truth. It is calculated as the ratio of the intersection area to the union area of the two regions. The dice coefficient is a widely used metric in image segmentation to quantify the similarity between the predicted segmentation and the ground truth. Similar to the IoU, the dice coefficient evaluates the degree of overlap between two regions, providing insight into the accuracy of the segmentation process. The dice coefficient is calculated using Equation (1).

$$Dice\ Coefficient = 2 \times \frac{Intersection}{Prediction\ Volume + Ground\ Truth\ Volume} \tag{1}$$

Here, the term "intersection" refers to the volume of overlapping voxels between the predicted segmentation and the ground truth, while "prediction volume" and "ground truth volume" represent the volumes of the respective regions.

Table 1. Performance comparison of the resection cavity segmentation model

Model Name	IOU	VAL_IOU	DICE_COEF	VAL_DICE_COEF
U-Net	0.6765	0.6772	0.7245	0.7144
Attention Enabled U-Net	0.8373	0.7718	0.8255	0.8136
U-Net with VGG16 Backbone	0.7934	0.7513	0.7752	0.7432
Proposed Model	**0.8901**	**0.8773**	**0.8933**	**0.8825**

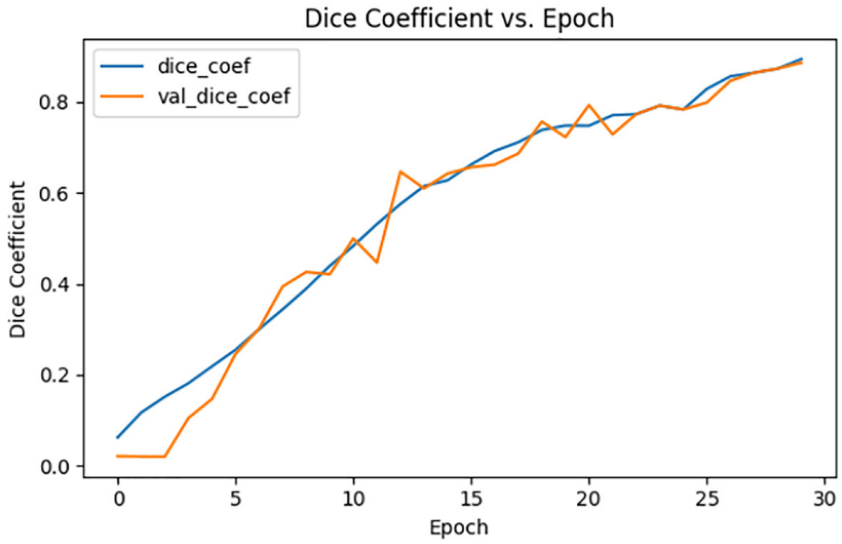

Fig. 7. *(Continued)*

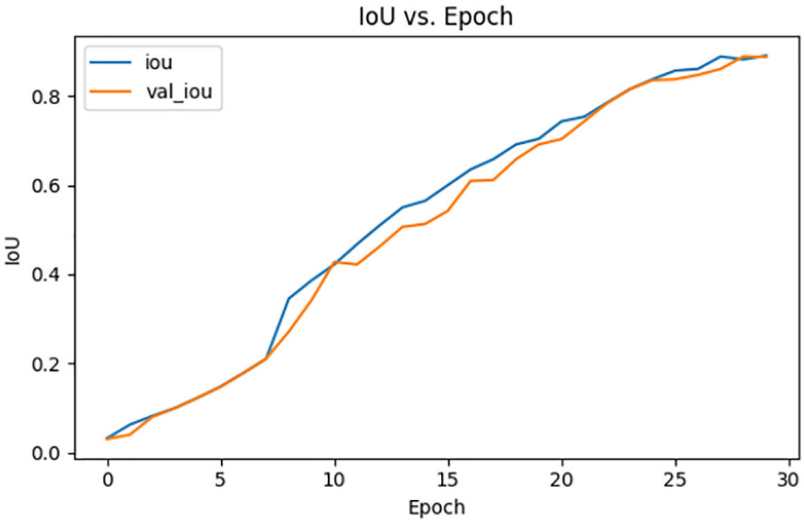

Fig. 7. Performance metrics of proposed model on EPISURG datasets

Table 1 and Figure 7 present the performance metrics of various models evaluated on the modified EPISURG dataset. The metrics include the Dice Coefficient and Intersection over Union (IoU). The results indicate that the proposed model performs favourably on the post-operative dataset. This demonstrates the model's effectiveness in accurately segmenting brain tumor regions across diverse datasets. In the evaluation of the proposed model's performance, its effectiveness was further examined using a clinical dataset consisting of 10 postoperative brain MRI cases. The dataset's results were analysed by assessing Hausdorff distances and MSD (mean surface distance) values. Specifically, the Hausdorff distances ranged from 0.02 to 0.12, while the MSD values ranged from 0.01 to 0.06. These metrics served as critical indicators of the model's accuracy in segmenting postoperative resection cavities. Smaller Hausdorff distances and MSD values signify improved segmentation accuracy, reflecting the model's proficiency in accurately delineating the boundaries of resection cavities within the MRI images. These findings affirm the model's reliability and competence in performing the complex task of postoperative resection cavity segmentation, a crucial aspect in the field of medical imaging analysis. The visual representation of these results, as depicted in Figure 8, highlights the model's ability to provide accurate and precise segmentation, confirming its potential for clinical application.

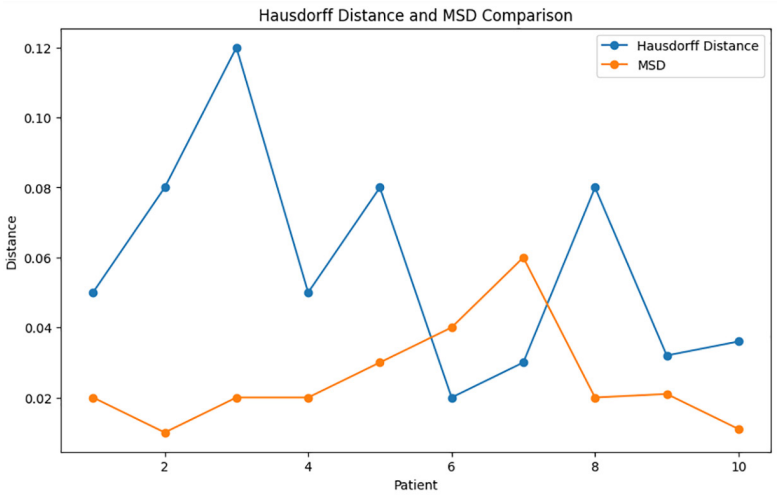

Fig. 8. Evaluation of the model on the clinical dataset using Hausdorff distance and MSD

6 DISCUSSION

This paper presents an automated deep learning model for resection cavity segmentation in postoperative brain MRI. Fully automated segmentation provides significant time advantages over manual and semi-automated methods [33]. This method has several key advantages. First, this model explicitly trains on postoperative brain MRI. Most of the existing methods utilize preoperative brain MRI segmentation models and fine-tune them to enable postoperative brain MRI segmentation. Secondly, to assess the effectiveness of the proposed model, an evaluation is conducted using clinical datasets that have been manually segmented by a radiologist. Third, this model provides a detailed comparison of preoperative and postoperative MRI images. The segmentation of resection cavities provides a detailed understanding of the anatomical changes. Comparative analysis of pre- and postoperative MRI contributes to improving clinical decision-making and patient outcomes.

Significant contributions to cavity segmentation have been made by the following researchers: Pérez-García et al. [20] employed a self-supervised 3D CNN for resection cavity (RC) segmentation and simulated resections in their study. The model achieved median dice similarity coefficients (DSCs) ranging from 74.9 to 82.4. Campbell Arnold et al. [2] introduced a modified U-Net model for cavity delineation, achieving a test median Dice-Sørensen coefficient (DSC) of 0.84 ± 0.08 and 0.74 ± 0.22 (median ± interquartile range). Additionally, Jungo et al. [18] attempted resection cavity segmentation in glioblastoma multiforme (GBM) patients. In their study, the classifier was explicitly trained on data from GBM patients, resulting in a classifier performance with a median DSC of 0.83. Unlike some of the existing methods that utilize preoperative brain MRI models and fine-tune them for postoperative MRI, our model is explicitly trained on postoperative brain MRI data. The utilization of VGG16 as the model's backbone is beneficial for handling limited datasets. Table 2. This section presents a comparison of various cavity segmentation models, including the proposed method, based on their median dice similarity coefficient.

Table 2. Comparison of existing cavity segmentation models vs. proposed model

Study Details	Model	Median DSC
Pérez-García et al. [20]	Self-supervised 3D CNN	0.82
Campbell Arnold et al. [2]	Modified U-Net model	0.84
Ermiş et al. [17]	Trained on GBM patient data	0.83
Proposed Method	Attention-enabled U-Net with VGG16	0.89

There are some inherent challenges in the study, such as the limited dataset size, which is often exacerbated by patients seeking treatment elsewhere post-surgery. Consequently, obtaining paired pre- and post-operative data remains a significant challenge. An effective data augmentation strategy becomes imperative to compensate for the scarcity of samples and enhance model robustness. Future efforts could focus on implementing a generative model to address the challenge of a limited dataset size. These endeavours aim to enhance the precision and adaptability of this segmentation technique for improved medical imaging analysis.

7 CONCLUSION

The study aims to improve post-operative MRI brain image segmentation, which is crucial for the care of brain tumour patients. It introduces the 'Attention-Enhanced VGG-U-Net' model, which utilizes the initial weights of VGG16 as the encoder base and integrates a self-attention module in the decoder. The model, trained on available post-operative MRI datasets, demonstrates a five-percentage point increase in Dice score compared to state-of-the-art CNN-based segmentation models. Additionally, a volumetric analysis of pre- and post-operative brain MRI scans provides valuable insights into surgical outcomes and follow-up treatments. Despite challenges with dataset size and availability, this research paves the way for future advancements, laying a foundation to enhance post-surgery care and brain tumour patient treatments.

8 REFERENCES

[1] N. Sanai and M. S. Berger, "Surgical oncology for gliomas: The state of the art," *Nature Reviews Clinical Oncology*, vol. 15, no. 2, pp. 112–125, 2018. https://doi.org/10.1038/nrclinonc.2017.171

[2] T. C. Arnold *et al.*, "Deep learning-based automated segmentation of resection cavities on postsurgical epilepsy MRI," *NeuroImage: Clinical*, vol. 36, p. 103154, 2022. https://doi.org/10.1016/j.nicl.2022.103154

[3] I. Despotović, B. Goossens, and W. Philips, "MRI segmentation of the human brain: Challenges, methods, and applications," *Computational and Mathematical Methods in Medicine*, vol. 2015, 2015. https://doi.org/10.1155/2015/450341

[4] M. Adamu Mohammed, O. Bismark, S. Alornyo, M. Asante, and B. Obo Essah, "ResFCNET: A skin lesion segmentation method based on a deep residual fully convolutional neural network," *IETI Transactions on Data Analysis and Forecasting (iTDAF)*, vol. 1, no. 1, pp. 4–19, 2023. https://doi.org/10.3991/itdaf.v1i1.35723

[5] A. Azeroual, Y. El Ouahabi, B. Nsiri, A. Dakil, M. H. El Yousfi Alaoui, A. Soulaymani, and B. Benaji, "Convolutional neural network for segmentation and classification of glaucoma," *International Journal of Online and Biomedical Engineering (iJOE)*, vol. 19, no. 17, pp. 19–32, 2023. https://doi.org/10.3991/ijoe.v19i17.43029

[6] T. A. Ton Komar Azaharan, A. K. Mahamad, S. Saon, Muladi, and S. W. Mudjanarko, "Investigation of VGG-16, ResNet-50 and AlexNet performance for brain tumor detection," *International Journal of Online and Biomedical Engineering (iJOE)*, vol. 19, no. 8, pp. 97–109, 2023. https://doi.org/10.3991/ijoe.v19i08.38619

[7] M. H. Hesamian, W. Jia, X. He, and P. Kennedy, "Deep learning techniques for medical image segmentation: Achievements and challenges," *Journal of Digital Imaging*, vol. 32, pp. 582–596, 2019. https://doi.org/10.1007/s10278-019-00227-x

[8] H. Lu, Y. She, J. Tie, and X. Xu, "Half-U-Net: A simplified U-Net architecture for medical image segmentation," *Frontiers in Neuroinformatics*, vol. 16, p. 911679, 2022. https://doi.org/10.3389/fninf.2022.911679

[9] L. Alzubaidi, J. Zhang, A. J. Humaidi, A. Al-Dujaili, Y. Duan, Al-Shamma, and L. Farhan, "Review of deep learning: Concepts, CNN architectures, challenges, applications, future directions," *Journal of Big Data*, vol. 8, pp. 1–74, 2021. https://doi.org/10.1186/s40537-021-00447-5

[10] O. Oktay *et al.*, "Attention u-net: Learning where to look for the pancreas," arXiv preprint arXiv:1804.03999, 2018. https://doi.org/10.48550/arXiv.1804.03999

[11] M. Hashemi, M. Akhbari, and C. Jutten, "Delve into multiple sclerosis (MS) lesion exploration: A modified attention U-net for MS lesion segmentation in brain MRI," *Computers in Biology and Medicine*, vol. 145, p. 105402, 2022. https://doi.org/10.1016/j.compbiomed.2022.105402

[12] I. R. I. Haque and J. Neubert, "Deep learning approaches to biomedical image segmentation," *Informatics in Medicine Unlocked*, vol. 18, no. 100297, 2020. https://doi.org/10.1016/j.imu.2020.100297

[13] K. Simonyan and A. Zisserman, "Very deep convolutional networks for large-scale image recognition," arXiv preprint arXiv:1409.1556, 2014. https://doi.org/10.48550/arXiv.1409.1556

[14] A. A. Pravitasari *et al.*, "U-Net-VGG16 with transfer learning for MRI-based brain tumor segmentation," *TELKOMNIKA (Telecommunication Computing Electronics and Control)*, vol. 18, no. 3, pp. 1310–1318, 2020. https://doi.org/10.12928/telkomnika.v18i3.14753

[15] R. Yousef, S. Khan, G. Gupta, T. Siddiqui, B. M. Albahlal, S. A. Alajlan, and M. A. Haq, "U-Net-Based models towards optimal MR brain image segmentation," *Diagnostics*, vol. 13, no. 9, p. 1624, 2023. https://doi.org/10.3390/diagnostics13091624

[16] N. Gharaibeh, A. Abu-Ein, O. M. Al-Hazaimeh, K. M. O. Nahar, W. A. Abu-Ain, and M. M. Al-Nawashi, "Swin transformer-based segmentation and multi-scale feature pyramid fusion module for Alzheimer's disease with machine learning," *International Journal of Online & Biomedical Engineering*, vol. 19, no. 4, pp. 22–50, 2023. https://doi.org/10.3991/ijoe.v19i04.37677

[17] K. Zeng *et al.*, "Segmentation of gliomas in pre-operative and post-operative multimodal magnetic resonance imaging volumes based on a hybrid generative-discriminative framework," in *Brainlesion: Glioma, Multiple Sclerosis, Stroke and Traumatic Brain Injuries: Second International Workshop, BrainLes 2016, with the Challenges on BRATS, ISLES and mTOP 2016, Held in Conjunction with MICCAI 2016*, Springer International Publishing, Athens, Greece, 2016, pp. 184–194. https://doi.org/10.1007/978-3-319-55524-9_18

[18] A. Jungo, R. Meier, E. Ermis, E. Herrmann, and M. Reyes, "Uncertainty-driven sanity check: Application to postoperative brain tumor cavity segmentation," arXiv preprint arXiv:1806.03106, 2018. https://doi.org/10.48550/arXiv.1806.03106

[19] K. Chang *et al.*, "Automatic assessment of glioma burden: A deep learning algorithm for fully automated volumetric and bidimensional measurement," *Neuro-oncology*, vol. 21, no. 11, pp. 1412–1422, 2019. https://doi.org/10.1093/neuonc/noz106

[20] F. Pérez-García *et al.*, "A self-supervised learning strategy for postoperative brain cavity segmentation simulating resections," *International Journal of Computer Assisted Radiology and Surgery*, vol. 16, no. 10, pp. 1653–1661, 2021. https://doi.org/10.1007/s11548-021-02420-2

[21] E. Lotan, B. Zhang, S. Dogra, W. D. Wang, D. Carbone, G. Fatterpekar, and Y. W. Lui, "Development and practical implementation of a deep learning–based pipeline for automated pre-and postoperative glioma segmentation," *American Journal of Neuroradiology*, vol. 43, no. 1, pp. 24–32, 2022. https://doi.org/10.3174/ajnr.A6872

[22] M. Holtzman Gazit, R. Faran, K. Stepovoy, O. Peles, and R. R. Shamir, "Post-operative glioblastoma multiforme segmentation with uncertainty estimation," *Frontiers in Human Neuroscience*, vol. 16, p. 932441, 2022. https://doi.org/10.3389/fnhum.2022.932441

[23] K. K. Ramesh *et al.*, "A fully automated post-surgical brain tumor segmentation model for radiation treatment planning and longitudinal tracking," *Cancers (Basel)*, vol. 15, no. 15, p. 3956, 2023. https://doi.org/10.3390/cancers15153956

[24] M. Ghaffari, G. Samarasinghe, M. Jameson, F. Aly, L. Holloway, P. Chlap, and R. Oliver, "Automated post-operative brain tumour segmentation: A deep learning model based on transfer learning from pre-operative images," *Magnetic Resonance Imaging*, vol. 86, pp. 28–36, 2022. https://doi.org/10.1016/j.mri.2021.10.012

[25] R. Billardello *et al.*, "Novel user-friendly application for MRI segmentation of brain resection following epilepsy surgery," *Diagnostics*, vol. 12, no. 4, p. 1017, 2022. https://doi.org/10.3390/diagnostics12041017

[26] R. F. Casseb, B. M. de Campos, M. Morita-Sherman, A. Morsi, E. Kondylis, W. E. Bingaman, and F. Cendes, "ResectVol: A tool to automatically segment and characterize lacunas in brain images," *Epilepsia Open*, vol. 6, no. 4, pp. 720–726, 2021. https://doi.org/10.1002/epi4.12468

[27] X. Li, P. S. Morgan, J. Ashburner, J. Smith, and C. Rorden, "The first step for neuroimaging data analysis: DICOM to NIfTI conversion," *Journal of Neuroscience Methods*, vol. 264, pp. 47–56, 2016. https://doi.org/10.1016/j.jneumeth.2016.02.017

[28] M. M. Gitonga, "Multiclass MRI brain tumor segmentation using 3D attention-based U-Net," arXiv preprint arXiv:2305.06203, 2023. https://doi.org/10.48550/arXiv.2305.06203

[29] A. A. Pravitasari *et al.*, "U-Net-VGG16 with transfer learning for MRI-based brain tumor segmentation," *TELKOMNIKA (Telecommunication Computing Electronics and Control)*, vol. 18, no. 3, pp. 1310–1318, 2020. https://doi.org/10.12928/telkomnika.v18i3.14753

[30] A. A. Asiri *et al.*, "Brain tumor detection and classification using fine-tuned CNN with ResNet50 and U-Net Model: A study on TCGA-LGG and TCIA dataset for MRI applications," *Life*, vol. 13, no. 7, p. 1449, 2023. https://doi.org/10.3390/life13071449

[31] E. I. Zacharaki, C. S. Hogea, D. Shen, G. Biros, and C. Davatzikos, "Non-diffeomorphic registration of brain tumor images by simulating tissue loss and tumor growth," *Neuroimage*, vol. 46, no. 3, pp. 762–774, 2009. https://doi.org/10.1016/j.neuroimage.2009.01.051

[32] B. Alexander *et al.*, "Desikan-Killiany-Tourville atlas compatible version of M-CRIB neonatal parcellated whole brain atlas: The M-CRIB 2.0," *Frontiers in Neuroscience*, vol. 13, p. 34, 2019. https://doi.org/10.3389/fnins.2019.00034

[33] O. Ronneberger, P. Fischer, and T. Brox, "U-net: Convolutional networks for biomedical image segmentation," in *Proceedings of Medical Image Computing and Computer-Assisted Intervention–MICCAI 2015: 18th International Conference*, Munich, Germany, 2015, pp. 234–241. https://doi.org/10.1007/978-3-319-24574-4_28

9 AUTHORS

Sobha Xavier P is a Research Scholar at the School of Engineering and Technology, Christ Deemed to be University, Bangalore Campus. She is also an Assistant Professor at the Department of Computer Science and Engineering at Jyothi Engineering College. Her primary research interests include Image Processing, Computer Vision, Data Science, Machine Learning, and Deep Learning (E-mail: sobha.xavier@res.christuniversity.in).

Sathish P K is an Associate Professor at the Department of Computer Science and Engineering at the School of Engineering and Technology, Christ Deemed to be University, Bangalore Campus. He holds a Ph.D. degree from Visvesvaraya Technological University, which he completed in 2019. He also has an AMIE certification and a Master's degree (MTech). His expertise lies in the fields of Computer Science, Artificial Intelligence, Image Processing, Computer Vision, and Pattern Recognition.

Raju G is a Professor at the Department of Computer Science and Engineering at the School of Engineering and Technology, Christ Deemed to be University, Bangalore Campus. He has a diverse educational background, with a Masters's degree in Physics, a Masters's degree in Computer Applications, and a Doctoral degree in Computer Science from the University of Kerala. Additionally, he completed his M. Tech in Computer Science and IT from Manonmaniam Sundaranar University, Tirunelveli. His primary research interests include Image Processing, Computer Vision, Data Science, Machine Learning, and Deep Learning. He has published over 120 research articles and has supervised 24 Ph.D. scholars.